A Re-examination of Molecular Bond Breaking Under Dynamic Forcing

Aaron L. Fogelson[*,+], Nathan Hancock[*], James P. Keener [*,+],
Rustem I. Litvinov [#], and John W. Weisel[#]

Departments of Mathematics[*] and Bioengineering[+]
155 South 1400 East, 233 JWB
University of Utah
Salt Lake City, Utah 84112

Department of Cell and Developmental Biology[#]
University of Pennsylvania
421 Curie Boulevard
Philadelphia, PA 19104

October 14, 2004

Classification: Biological Sciences: Biophysics and Physical Sciences: Applied Mathematics

Corresponding author:
Aaron Fogelson
Department of Mathematics
155 South 1400 East, 233 JWB
University of Utah
Salt Lake City, Utah 84112
email: fogelson@math.utah.edu, phone: (801) 581-8150, fax: (801) 581-4148

Abstract word count: 168
Paper character count:
Pages: 17, Figures: 7, Tables: 0

Abstract

Simple mathematical models are used to explore the rupture of molecular bonds subject to a dynamically increasing force as applied in optical trapping and atomic force microscopy experiments. The Markov-equation-based theory proposed by Evans and Ritchie (Biophys. J., 1997, 72, 1541-1555) assumes that the unbinding rate grows exponentially with the applied force and predicts a logarithmic dependence of rupture force on the loading rate, *i.e.*, the rate at which the applied force is increased. In the current paper, simulations using Fokker-Planck-based models show that the rupture force is a biphasic function of loading rate, even for a single-well binding potential. A Markov model that uses an appropriate unbinding rate can accurately capture this behavior. The appropriate unbinding rate can be tabulated by solving a sequence of steady-state Fokker-Planck equations for unbinding under constant force. As a function of force, this unbinding rate grows much more slowly than exponentially, and the rupture forces consistent with it are substantially larger than those predicted by the Evans and Ritchie theory.

Introduction

The ability of bonds between macromolecules to withstand external forces is critical throughout biology. Important examples involve the adhesion of cells in the blood (e.g., leukocytes, platelets, tumor cells) to the vascular wall and to one another. In particular, during platelet aggregation, the dimeric plasma protein fibrinogen binds to activated $\alpha_{IIb}\beta_3$ integrin receptors on the surfaces of two different platelets, and forms a molecular bridge between the platelets. The number of such bridges and the strength of each one are important factors in determining whether the platelets remain together in the background shear flow, and so influence whether a wall-bound platelet thrombus grows and how large it gets.

Using optical tweezers, atomic force microscopy, and other techniques, a large number of studies of bond strength have been carried out (see [16] and references therein). In these studies it is not possible to suddenly impose a constant force on the bond. Instead the applied force ramps up in time, and the rate of increase of the applied force is called the loading rate. Evans and Ritchie (E-R) [3, 5] proposed a theory to understand experiments of this kind, and made the important observation that the measured force at which the bond ruptures should depend on the loading rate. Further, their theory predicted that the rupture force should increase logarithmically as loading rate increases.

Weisel and coworkers used laser-tweezers (See Fig.1) to study the strength of the fibrinogen-$\alpha_{IIb}\beta_3$ bond [12]. They measured rupture forces for a range of loading rates (160 pN/sec to 16,000 pN/sec) of physiological interest. At each loading rate, a distribution of rupture forces was measured over many experiments; the peak of this distribution (approximately 85 pN) changed very little as the loading rate varied, indicating that the rupture force for this bond has little sensitivity to loading rate at least over the range of physiologically relevant loading rates. Thus, Weisel's results seem to disagree with the predictions of the E-R theory. Some experimental studies of bond rupture for different molecular systems report logarithmic dependence over the full range of loading rates studied [9] or piecewise logarithmic dependence with different slopes in different intervals of loading rates [4, 13, 15, 17]. Other studies report little sensitivity to loading rate [2] or other non-logarithmic dependence [8]. In some cases, complex models have been proposed to account for the non-logarithmic behavior [8]. Because of the range of results, including a number that are at odds with the existing theory, in this paper we re-examine the breaking of molecular bonds under dynamic forcing. We find that while there is a range of loading rates over which the rupture force indeed depends logarithmically on loading rate, this range is sometimes quite limited, and so characterizing the overall dependence as 'logarithmic' is misleading. Even in the logarithmic range, the rupture forces predicted by the E-R theory can be substantially in error. We also find that, even for very simple models, it is common that there is a substantial range of loading rates

over which the rupture force is quite insensitive to loading rate.

The E-R theory is based on a Markov model $dP/dt = -k_{\rm off}P$ for the probability $P(t)$ that the bond is intact at time t, in which, following Bell [1], it is assumed that the unbinding rate $k_{\rm off}$ is an exponential function of the instantaneous external force F applied to the molecule. That is, $k_{\rm off}(F) = k_0 \exp(F/F_0)$, where k_0 and F_0 are appropriate (F-independent) scale factors. By looking at Langevin and Fokker-Planck (F-P) equation descriptions of the unbinding process, we find that this choice of off-rate is often inappropriate. We also show that using a Markov model with an off-rate tabulated by solving the appropriate steady-state F-P equation with constant applied force, there is good agreement with the predictions from the time-dependent F-P equation that describes unbinding under dynamic forcing.

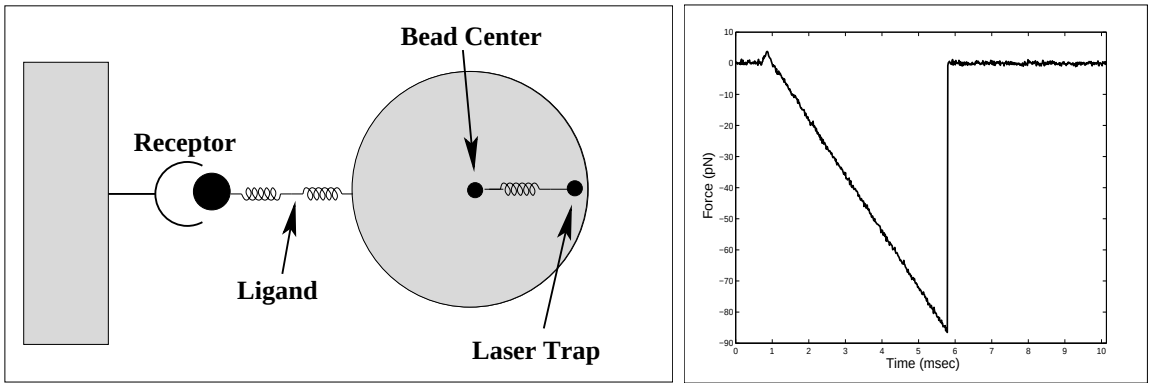

Figure 1: Left: Schematic of laser tweezers system. Fibrinogen molecules and $\alpha_{IIb}\beta_3$ molecules are attached at low density to, respectively, a 1μm diameter latex bead and the surface of a stationary pedestal. The laser tweezers are used to move the bead toward the pedestal and then to pull it away. The laser is moved at a prescribed velocity and the distance between the center of the beam and the center of the bead is measured. Using this distance and the effective spring constant for the laser-bead system, the force applied by the laser to the bead at each instance of time is computed. Right: Schematic of rupture force measurement. The slight upward bump in the graph near time 1 indicates contact of the bead and the pedestal. The laser's force on the bead increases approximately linearly as the beam is moved to pull the bead away from the pedestal and then drops drastically when the bond ruptures.

Three Variable Model

The first model we consider involves Langevin equations for the positions of the bead center $X(\tau)$, the ligand head $Y(\tau)$, and the center of the laser beam $Z(\tau)$ as functions of time τ:

$$\nu_X dX(\tau) = k_l(Z - X)d\tau - k_s(X - Y - r_0)d\tau, \tag{1}$$

$$\nu_Y dY(\tau) = -F_b d\tau + k_s(X - Y - r_0)d\tau + \sqrt{k_B T \nu_Y d\tau}\; dW(0,1), \tag{2}$$

$$dZ(\tau) = \frac{v}{k_l} d\tau. \tag{3}$$

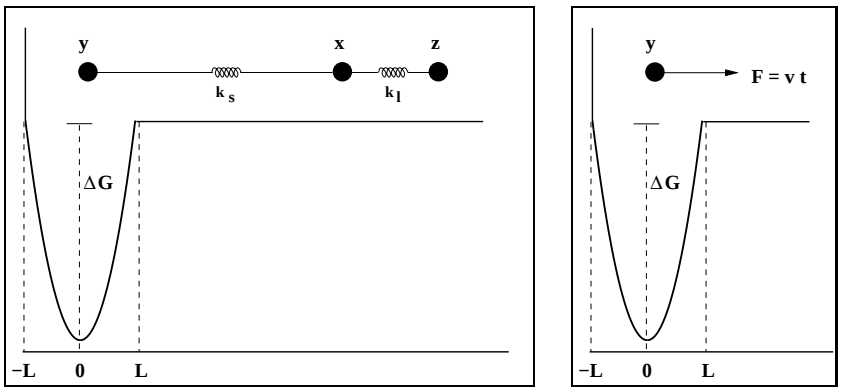

Figure 2: Model Schematic: Left, three variable model. Right, one variable model.

These equations correspond to the schematic diagram in the left panel of Fig.2, and we note that because of the small size of the objects involved we have ignored mass. Here, ν_X and ν_Y are the friction coefficients for the bead and ligand head, respectively; k_s and k_l are the spring constants for the ligand molecule and laser trap, respectively; r_0 is the distance between the bead center and ligand molecule head when the molecule is unstressed; k_B is Boltzmann's constant; T is the absolute temperature; F_b is the force due to the binding potential; dW are Gaussian steps with mean 0 and variance 1; and v is the loading rate for the laser trap system. Only the thermal motion of the ligand molecule is included in the equations as the random motion of the bead is negligible by comparison.

Throughout this paper, the bond potential force is assumed to come from a potential that is quadratic for $-L < Y < L$ and constant for $Y > L$. For simulations, the transition at $Y = L$ is smoothed using a cutoff function, so the force is given by $F_b = (F_{\max} Y/L)H(Y)$ where $H(Y) = 1/2(1 - \tanh(\gamma(Y - L))$ is the cutoff function ($\gamma > 0$ is constant), L is the width of the potential well, and $\Delta G = F_{\max} L/2$ is the well depth. $Y(t)$ is restricted to being larger than $-L$ by use of reflective boundary condition at $-L$. This restriction has no significant effect on the behavior of

the model system for the parameters and situations we studied, as $Y(t)$ almost never approaches $-L$.

The model given by Eqs.(1-3) contains a number of parameters, for some of which reasonable values can be obtained from the literature. Specifically, we use the value $k_l = 0.2$ pN/nm measured by Weisel, we compute the bead friction coefficient to be $\nu_X \approx 0.19 \cdot 10^{-4}$ pN sec/nm using Stokes' formula for the drag on a sphere of radius 1μm moving at low Reynolds number in water, and we use $k_B T = 4.3$ pN nm [11]. For the molecular friction coefficient ν_Y, we use the value $0.6 \cdot 10^{-7}$ pN sec/nm given by [11] for the drag coefficient of a globular protein. We adjust k_s so that the extension of the ligand molecule is at most a few percent of its unstressed length, and find that values of k_s of 4.0 pN/nm or more are sufficient to achieve this.

We explore how the system behaves for different loading rates v and well depths ΔG. Realizations of solution paths for these equations are computed as described in Appendix 1. For each realization, we compute the maximum of the force $k_l(Z(\tau) - X(\tau))$ that would be measured experimentally. We define the rupture force as the mean of these maximum forces over the ensemble of simulated realizations. Results are shown in Fig.3 where we have plotted the mean rupture force against the loading rate on a logarithmic scale. We see that for a wide range of loading rates (including those used in Weisel's experiments), the rupture force shows very little sensitivity to the loading rate. We also see that there is a stark transition in the system's behavior so that at sufficiently high loading rates, the rupture force is very sensitive to loading rate. The transition occurs when the rupture force is the order of magnitude of the maximum force ($F_{\max}$) associated with the well potential. We also see that rupture forces of a magnitude similar to those measured by Weisel can be obtained for reasonable parameter choices.

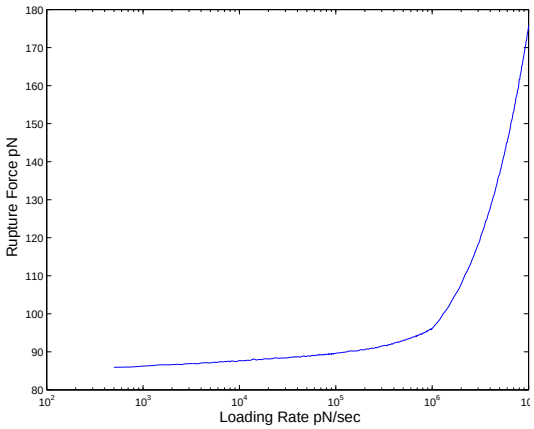

Figure 3: Rupture force vs. Loading Rate for the Model (1-3) for $\Delta G/(k_B T) \approx 250$.

One Variable Model

The second model we consider is a simplification of the model (1-3). We now imagine that the laser tweezers is able to apply a linearly increasing force directly to the molecule head (See Fig.2, right panel). The single equation of this model is for the position of the ligand molecule head and is $\nu_Y dY(\tau) = (-F_b + v\tau)d\tau + \sqrt{k_B T \nu_Y d\tau}\; dW(0,1)$, where the variables and parameters have the same meaning as earlier. It is useful to nondimensionalize this equation. We introduce nondimensional variables y and t defined by $Y = Ly$ and $\tau = \frac{L^2 \nu_Y}{(k_B T)} t$, and obtain the nondimensional Langevin equation

$$dy(t) = (-2ayH(y) + Vt)dt + \sqrt{dt}\; dW(0,1), \tag{4}$$

where $H(y)$ is the cutoff function in the scaled variables, and $a = \Delta G/(k_B T) = F_{max} L/(2k_B T)$ and $V = v(L^3 \nu_Y/(k_B T)^2$ are the non-dimensional well-depth and loading rate, respectively. The rupture force here is defined as the product of V and the ensemble average of the first time that a particle reaches $y = 1$.

Associated with the Langevin equation (4) is the F-P equation [6]:

$$p_t = -J_y = \{(2ay - Vt)p\}_y + p_{yy}. \tag{5}$$

where J is the probability flux defined by $J = (Vt - 2ay)p - p_y$. We consider the F-P equation for positions within the well, $-1 < y < 1$, and impose the no flux condition $J = 0$ at $y = -1$, and the absorbing boundary condition $p = 0$ at $y = 1$. For simulations, the initial data are taken to come from an approximate δ-function centered at the well center $y = 0$. The solution to the F-P system is computed using the finite-difference method described in Appendix 2. For the F-P simulations, the rupture force is defined as the product of the loading rate V and the mean first exit time $M(0)$ through the absorbing boundary at $y = 1$ for a particle beginning at $y = 0$, that is $F = VM(0)$. As a check on the numerical schemes for both the Langevin equations and the F-P equation, rupture forces over a wide range of loading rates were compared and found to be in excellent agreement (not shown). Note that the mean first exit time for a F-P equation with *time-dependent* potential can be calculated from the solution $p(y, t|0, 0)$ to the F-P equation as shown in Appendix 3.

The simpler model behaves qualitatively much like the first model. As shown in Fig.4, for each nondimensional well depth a, there is a wide range of nondimensional loading rates V over which the rupture force shows very little sensitivity to V. Again, for very high values of V there is a substantially different behavior; for this simpler model, the rupture force grows as $V^{1/2}$ for large V.

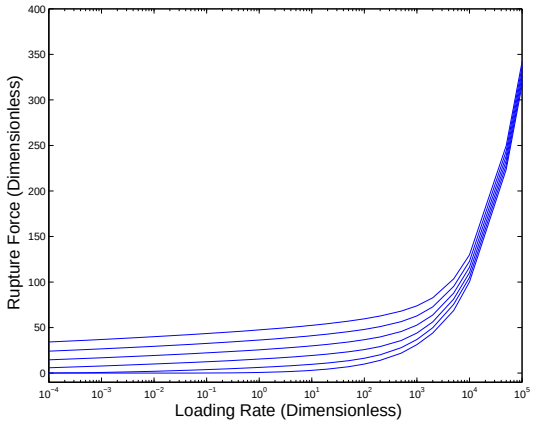

Figure 4: Rupture force $VM(0)$ vs. Loading Rate V calculated from the mean-exit time $M(0)$ for the Fokker-Planck equation (5) for well depths $a = \Delta G/(k_B T) = 1$, 11, 21, 31, 41, and 51 (bottom to top).

Markov Models

Simulations with Langevin or Fokker-Planck models can be expensive, so Markov models are often used to approximate their behavior. For the one-variable model described by (4) or (5), consider the Markov model:

$$\frac{dP}{dt} = -k_{\text{off}} P, \tag{6}$$

where $P(t)$ is the probability that the ligand is bound to the receptor at time t, and we have ignored the possibility of rebinding. The accuracy of the Markov model in approximating the other models depends on the choice of the off-rate k_{off}. It also depends on whether the time scale on which statistical equilibrium is reached in (4) or (5) is fast compared to the time scale on which k_{off} changes.

It is often assumed [1, 4, 13, 14] that the off-rate has the form

$$k_{\text{off}}(F) = k_0 \exp(F/F_0), \tag{7}$$

where F is the applied force, and k_0 and F_0 are appropriate scale factors. This assumption is motivated by the classical Arrhenius formula, namely that the off-rate for a chemical bond is

$$k_{\text{off}} = \kappa_0 \exp\left(-\frac{\Delta G}{k_B T}\right). \tag{8}$$

where ΔG is the free energy of the bond, *i.e.*, the height of the potential well out of which the bound molecule must escape. The idea leading from (8) to (7) is that an applied force 'tilts' the potential, changing the height of the barrier that the molecule must cross to unbind by an amount FL where L is the width of the well (for a quadratic well). According to this reasoning, the off-rate from the modified potential well should be

$$k_{\rm off}(F) = \kappa_0 \exp(-\frac{\Delta G - FL}{k_B T}) = k_0 \exp(\frac{FL}{k_B T}). \tag{9}$$

We contend that (9) is a poor choice of off-rate to use in a Markov model when FL approaches ΔG. To support this statement, we examine the F-P equation for a molecule subject to three forces: the force from the potential well, a *constant* applied force F, and Brownian forcing:

$$p_t = \{(2ay - f)p\}_y + p_{yy}. \tag{10}$$

Here $p(y,t)$ is the probability density that the particle is at y at time t, $U(y) = ay^2$ is the binding potential, and $a = \Delta G/(k_B T)$ and $f = FL/(k_B T)$ are the non-dimensional well-depth and applied force, respectively. Here we suppose that the binding site is contained in the interval $-1 < y < 1$, that the boundary $y = -1$ is reflecting, and that the boundary $y = 1$ is absorbing. The off-rate is the reciprocal of the mean first exit time, that is, the mean time for a particle to reach the absorbing boundary $y = 1$ having started at the minimum of the potential at $y = 0$. This is the appropriate off-rate to use in a Markov model of this process provided that statistical equilibrium is reached quickly. To explore how rapidly equilibrium is achieved for (10), we added a source term localized at $y = 0$ to balance any flux of p past $y = 1$. With f constant, the problem quickly reached equilibrium. We stepped f to a new value and observed that the system reequilibrated in times much shorter than the scale on which the external forcing in (5) varied.

Turning to the determination of the mean first exit time for (10), we recall that for an autonomous process, that is, one in which the applied force and potential are independent of time, the mean first exit time $M(y)$ for a particle starting at y is given by the solution of the ordinary differential equation

$$M'' - (2ay - f)M' = -1 \tag{11}$$

subject to the boundary conditions $M'(-1) = 0$ and $M(y) = 0$ [6]. (An efficient way to solve this problem is described in Appendix 4.) In Fig.5 we plot this off-rate as a function of well depth for the case that the applied force f is zero. We also plot the off-rate predicted by the Arrhenius formula, and it is evident that unless $a \equiv \Delta G/(k_B T) >> 1$, the two results differ substantially.

For a less than 5, the Arrhenius formula predicts a value at least an order of magnitude too large, and, in fact, as $a \to 0$, the Arrhenius value is more than two orders of magnitude too large.

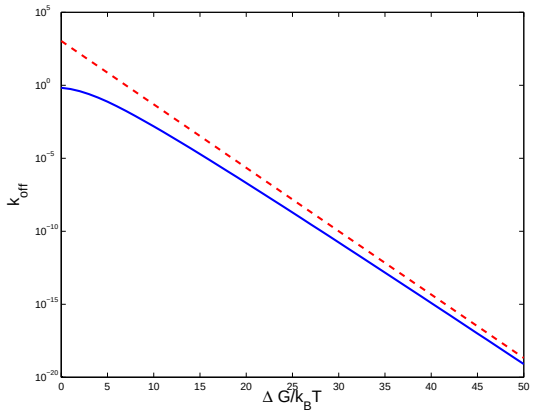

Figure 5: Plot of k_{off} (solid curve) and $\kappa_0 \exp(-\Delta G/(k_B T))$ (dashed curve), on a logarithmic scale, plotted as functions of $a = \Delta G/(k_B T)$.

The fact that the Arrhenius formula gives a poor approximation for small a makes it not surprising that under a constant force, the off-rate does *not* have the exponential dependence on force given in (9). This is illustrated in Fig.6 in which the actual off-rate determined by solving (11) is plotted as a function of $f \equiv (FL)/(k_B T)$ for several values of the well depth a. For small f the curves are nearly linear (at least for a sufficiently large), which indicates that for large enough a and small enough f, the effect of force on the off-rate is approximately exponential. But this is only valid for f significantly less than a, and in these portions of the curves, the off-rate is minuscule. The off-rate becomes significant when f approaches a and then the exponential-dependence formula *substantially* over-estimates the rate of unbinding, sometimes by many orders of magnitude.

The Markov model can give a good approximation to the rupture forces calculated from the F-P equation but only if the appropriate off-rate is used. One way to do this is to tabulate the off-rates obtained by solving (11) for a range of well-depths and forces, and to use these (interpolated appropriately) in a numerical solution of the Markov model. That is, in any timestep of the numerical solution of (6), use the tabulated off-rate appropriate for the well-depth and the instantaneous value of the force $F = Vt$.

Fig.7 shows results of this process along with rupture forces predicted using the exponential off-rate formula (7) in a Markov model, and the rupture forces predicted by the F-P model (5). Two things are evident: From the left panel we see that the Markov model with the correct off rate

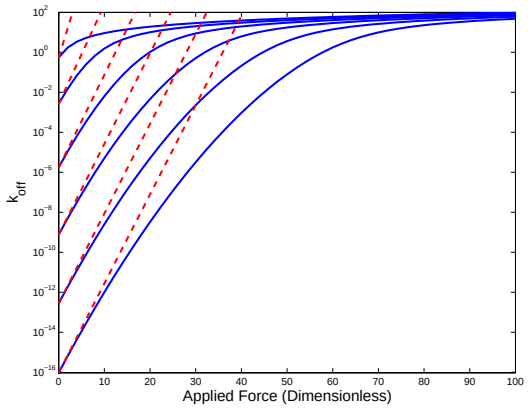

Figure 6: Solid curves show $k_{\rm off}$, on a logarithmic scale, as a function of $f = FL/(k_BT)$, for well depths $a = \Delta G/(k_BT) = 1$, 11, 21, 31, 41, and 51 (top to bottom). Dashed lines show the off-rate predicted by the exponential expression (7) with k_0 and F_0 chosen so each dashed line has the same value and slope as the corresponding solid curve at $F = 0$.

predicts rupture forces in good agreement with the F-P model. From the right panel, we see that with the exponential off-rate the Markov model predicts rupture forces that are quantitatively and qualitatively different than those computed from the F-P equation.

Conclusion

By comparison with solutions to Fokker-Planck and Langevin models for molecular unbinding under dynamic forcing, we show that a Markov model with an appropriate unbinding rate $k_{\rm off}$ can give accurate predictions of how the mean rupture force varies with the loading rate. The appropriate unbinding rate can be obtained by solving boundary value problems for the mean breaking time for a bond subject to constant force. On the other hand, a Markov model, such as the one proposed in [3, 5], that assumes the unbinding rate grows exponentially with the applied force, substantially overestimates the unbinding rate at each force and substantially underestimates the mean rupture force, especially for bonds characterized by deep potential wells. The use of such Markov models for interpreting experimental unbinding data, which has become fairly standard, needs to be re-thought in view of these observations.

Markov models based on the exponential off-rate predict an (approximately) logarithmic dependence of mean rupture force on loading rate for a single-well binding potential. In practice, experimental data for rupture force versus the logarithm of loading rate usually do not lie along a single line, but often seem to lie on different lines for different portions of the loading rate range

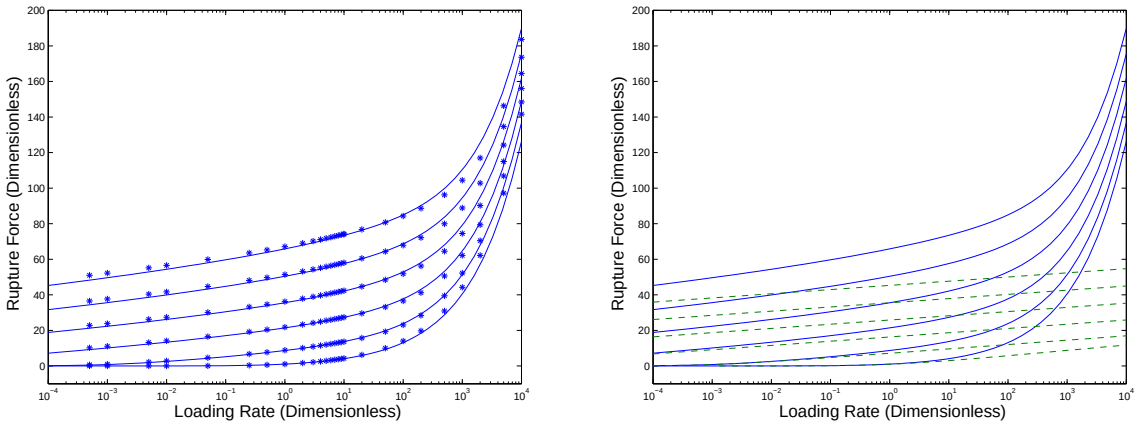

Figure 7: Rupture force vs. Loading rate. Left: Comparison of rupture forces predicted by the Fokker-Planck equation (*) and the Markov model (solid curve) with the correct off-rates determined by interpolating tabulated off-rate values from the solution of solving (11). Right: Comparison of rupture forces predicted by Markov model with the correct off rate (solid curve) and with the exponential off-rate (dashed curve). In both panels, curves from bottom to top correspond to well-depths a =1, 11, 21, 31, 41, and 51. The solution for the exponential off-rate was computed from the analytic formula for the mean first-exit time [8, 15].

investigated. For such multi-phasic cases, two or more different logarithmic functions are fit to the data, with each function used for a subset of loading rates. Each of the logarithmic functions is interpreted as corresponding to a distinct well through which the system must pass on the way to unbinding. In some cases, this interpretation has been corroborated by further experiments in which the addition of an inhibitor eliminates one of the phases in the data (*e.g.*, [4]. Our results suggest that this approach should be used with caution. Look, for example, at the top curve in Fig.(7), imagine that a half dozen or so data points were taken in the loading rate range 10^{-1} to 10^4. It would be tempting to fit them using two straight line segments, that is, by two different logarithmic functions of loading rate and to infer that these correspond to two energy wells. Yet this data comes from a binding potential with a single well, so such an inference would be incorrect. The problem is that the appearance of multi-phasic data does not necessarily imply a multi-well binding potential.

Appendix 1: Numerical Solution of Langevin Equation

Solutions of the Langevin equations are approximated numerically using the simple Euler scheme [10]. Letting X^n denote an approximation to $X(\tau)$ at time $\tau = n\Delta\tau$, and using similar notation for the other variables, the scheme is:

$$X^{n+1} = X^n + \frac{k_l}{\nu_X}(Z^n - X^n)\Delta\tau - \frac{k_s}{\nu_X}(X^n - Y^n - r_0)\Delta\tau \tag{12}$$

$$Y^{n+1} = Y^n - \frac{F_b^n}{\nu_Y}\Delta\tau + \frac{k_s}{\nu_Y}(X^n - Y^n - r_0)\Delta\tau + \left(\frac{2k_BT\Delta\tau}{\nu_Y}\right)^{1/2} G(0,1) \tag{13}$$

$$Z^{n+1} = Z^n + \frac{v}{k_l}\Delta\tau \tag{14}$$

with $F_b^n = F_{\max}(Y^n/2L)(1-\tanh(\gamma(Y^n - L))$. In (13), $G(0,1)$ denotes a Gaussian random variable with mean 0 and variance 1. For each simulation, N sample paths are followed and used to derive statistics. N is chosen to be sufficiently large that statistics are meaningful, and the timestep $\Delta\tau$ is chosen to be sufficiently small that further reductions in it cause negligible changes. The parameter γ is chosen so that the cutoff occurs over a distance small compared with the well-width L.

Appendix 2: Numerical Solution of Fokker-Planck Equation

Consider the Fokker-Planck equation (10) on $-1 \le y \le 1$ with no-flux boundary condition at $y = -1$ and absorbing boundary condition $p = 0$ at $y = 1$. Let $y_i = i\Delta y$ for $i = -I, -I+1, \ldots, I$ where $I\Delta y = 1$, and denote by p_j^n an approximation to the average of $p(y,t)$ over the i^{th} cell $y_i - \Delta y/2 \le y < y_i + \Delta y/2$ at time $t_n = n\Delta t$. (p_{-I}^n is the average over the half-cell $[-1, -1+\Delta y/2]$). The flux has an advective part $A = (Vt - 2ay)p$ and a diffusive part $-p_y$. We use a conservative difference approximation to (10) in which the diffusive flux across the right end $y_{i+1/2}$ of the i^{th} cell is approximated by the centered-difference quotient $-p_y \approx -(p_{i+1} - p_i)/\Delta y$ and the advective flux is approximated by the upwind formula:

$$A_{i+1/2}^n = \begin{cases} (Vt_n - 2ay_{j+1/2})p_i^n & (Vt_n - 2ay_{i+1/2}) > 0 \\ (Vt_n - 2ay_{j+1/2})p_{i+1}^n & (Vt_n - 2ay_{i+1/2}) < 0. \end{cases}$$

For the diffusive terms we use Crank-Nicolson time discretization while for the advective terms we use an explicit formulation. The resulting formula for p_i^{n+1} for $i = -I+1, \ldots, I-1$ is

$$\frac{p_i^{n+1} - p_i^n}{\Delta t} = \frac{1}{\Delta y}\left(A_{i-1/2}^n - A_{i+1/2}^n\right) + \frac{1}{\Delta y^2}\left(p_{i-1}^{n+1} - 2p_i^{n+1} + p_{i+1}^{n+1} + p_{i-1}^n - 2p_i^n + p_{i+1}^n\right). \tag{15}$$

The equation for $i = -I$ is somewhat different because of the boundary condition $J = 0$ at $y = -1$, and because the p^n_{-I} is the average over a cell of width $\Delta y/2$. For $i = I$, we set $p^n_I = 0$ for all n to enforce the absorbing boundary condition there.

Appendix 3: Mean First Exit Time with a Time-dependent Potential

The mean first exit time for a Fokker-Planck system with a time-*independent* potential is usually calculated by solving a boundary value problem derived from the associated backward Fokker-Planck equation [6]. This approach does not extend to time-dependent potentials, so here we show how to determine the mean first exit time from the solution of the forward Fokker-Planck equation for a problem with a time-dependent potential.

For the domain $\Omega = \{y : -1 < y < 1\}$, consider the Fokker-Planck equation $p_t = -J_y$, where $p = p(y, t|y', t')$ is the probability of finding a particle at location y at time t given that it was at position y' at time t'. The boundary conditions are $J = 0$ at $y = -1$ and $p(1, t|y', t') = 0$. Define $G(y, t) = \int_{-1}^{1} p(x, t|y, 0)dx$ and observe that if $\mathcal{T}(y)$ is the random variable for the time at which a particle that starts at y leaves the domain Ω, then $\Pr(\mathcal{T}(\mathrm{y}) > \mathrm{t}) = \mathrm{G(y, t)}$. Set $g(y, t) = -G_t(y, t)$, and note that $\Pr(\mathcal{T}(\mathrm{y}) > \mathrm{t}) = \int_{\mathrm{t}}^{\infty} \mathrm{g(y, s)ds}$ and $\Pr(\mathcal{T}(\mathrm{y}) < \mathrm{t}) = \int_{0}^{\mathrm{t}} \mathrm{g(y, s)ds}$, so that $g(y, t)$ is the probability distribution function for the random variable $\mathcal{T}(y)$. Hence one expression for the mean first exit time $M(y)$ is

$$M(y) = \int_0^\infty t g(y, t)dt = \int_0^\infty t \int_{-1}^{1} p(x, t|y, 0)dxdt. \tag{16}$$

Here, $p(x, t|y, 0)$ can be found by solving $p_t = -J_y$ with initial condition $p(x, 0|y, 0) = \delta(x - y)$. By noting that $g(y, t) = -\int_{-1}^{1} p_t(x, t|y, 0)dx = \int_{-1}^{1} J_x(p(x, t|y, 0))dx = J(p(1, t|y, 0))$, we obtain a second expression for $M(y)$:

$$M(y) = \int_0^\infty s J(p(1, s|y, 0))ds. \tag{17}$$

In computations, we use discrete analogues of both (16) and (17) and continue our simulations until such time that the maximum of $p(y, t|0, 0)$ for $y \in \Omega$ is less than a small tolerance. At that time, the two expressions for $M(0)$ give values that are essentially equal, as is expected with the conservative scheme we use to solve the Fokker-Planck equation.

Appendix 4: Solution of Equation (11).

An analytic solution of Eq(11) with the boundary conditions $M'(-1) = 0$ and $M(1) = 0$ can be derived easily but it complicated to evaluate and is therefore not particularly useful. A straightforward way to solve the problem is to write (11) as a system of first-order differential equations

$$M'(y) = N(y), \tag{18}$$

$$N'(y) = (2ay - f)N(y) - 1. \tag{19}$$

Solving this system with conditions $M(-1) = 0$ and $N(-1) = 0$ gives a function, call it $M_0(y)$, which satisfies (11) and the boundary condition $M'(-1) = 0$, but not the boundary condition $M(1) = 0$. The function $M(y) = M_0(y) - M_0(1)$ satisfies (11) and the boundary conditions at both $y = -1$ and $y = 1$. Numerical solutions to the system (18-19) for $-1 \leq y \leq 1$ with the 'initial conditions' $M(-1) = N(-1) = 0$ are easily computed using any standard method for stiff ordinary differential equations [7].

Acknowledgments: This work was supported in part by NSF FRG DMS-0139926. NH was supported in part by an REU award from NSF VIGRE grant DMS-0091675.

References

[1] George I. Bell. Models for the specific adhesion of cells to cells. *Science*, 200:618–627, 1978.

[2] Xian-E Cai and Jie Yang. The binding potential between the cholera toxin B-oligomer and its receptor. *Biochemistry*, 42:4028–4034, 2003.

[3] Evan Evans. Probing the relation between force – lifetime – and chemistry in single molecular bonds. *Annu. Rev. Biophys. Biomol. Struct.*, 30:105–128, 2001.

[4] Evan Evans, Andrew Leung, Dan Hammer, and Scott Simon. Chemically distinct transition states govern rapid dissociation of single L-selectin bonds under force. *PNAS*, 98(7):3784–3789, 2001.

[5] Evan Evans and Ken Ritchie. Dynamic strength of molecular adhesion bonds. *Biophys. J.*, 72:1541–1555, 1997.

[6] C.W. Gardiner. *Handbook of Stochastic Methods*. Springer, New York, NY, 1997.

[7] C. W. Gear. *Numerical Initial Value Problems in Ordinary Differential Equations*. Prentice-Hall, Englewood Cliffs, NJ, 1971.

[8] C. Gergely, J. Hemmerle, P. Schaaf, J.K H. Horber, J-C Voegel, and B. Senger. Multi-bead-and-spring model to interpret protein detachment studied by afm force spectroscopy. *Biophys. J.*, 83:706–722, 2002.

[9] William D. Hanley, Denis Wirtz, and Konstantinos Konstantopoulos. Distinct kinetic and mechanical properties govern selectin-leukoeyte interactions. *J. Cell Sci.*, 117:2503–2511, 2004.

[10] Desmond J. Higham. An algorithmic introduction to numerical simulation of stochastic differential equations. *SIAM Review*, 43:525–546, 2001.

[11] Jonathan Howard. *Mechanics of Motor Proteins and the Cytoskeleton*. Sinauer, Sunderland, MA, 2001.

[12] R.I. Litvinov, H. Shuman, J.S. Bennett, and J.W. Weisel. Binding strength and activation state of single fibrinogen-integrin pairs on living cells. *PNAS*, 99:7426–7431, 2002.

[13] R. Merkel, R. Nassoy, A. Leung, K. Ritchie, and E. Evans. Energy landscapes of receptor-ligand bonds explored with dynamic force spectroscopy. *Nature*, 397:50–53, 1999.

[14] Chase E. Orsello, Douglas A. Lauffenburger, and Daniel A. Hammer. Molecular properties in cell adhesion: a physical and engineering perspective. *TRENDS Biotech.*, 19(8):310–316, 2001.

[15] David F. J. Tees, Richard E. Waugh, and Daniel A. Hammer. A microcantilever device to assess the effect of force on the lifetime of selectin-carbohydrate bonds. *Biophys. J.*, 80:668–682, 2001.

[16] John W. Weisel, Henry Shuman, and Rustem I. Litvinov. Protein-protein unbinding induced by force: Single-molecule studies. *Curr. Opin. Struct. Biol.*, 13:227–235, 2003.

[17] X. Zhang, E. Wojcikiewicz, and V.T. Moy. Force spectroscopy of the leukocyte function-associated antigen-1/intercellular adhesion molecule-1 interaction. *Biophys. J.*, 83:2270–2279, 2002.